Supplementary Information

# Parallel dilution microfluidic device for enabling logarithmic concentration generation in molecular diagnostics

Akira Miyajima*[a], Fumiya Nishimura[a], Daigo Natsuhara[bc], Yuka Kiba[d], Shunya Okamoto[a], Moeto Nagai[ae], Tadashi Yamamuro[f], Masashi Kitamura[d] and Takayuki Shibata*[ae]

[a] *Department of Mechanical Engineering, Toyohashi University of Technology, 1-1 Hibarigaoka, Tempaku-cho, Toyohashi, Aichi 441-8580, Japan.*

[b] *Institute for Advanced Research (IAR), Nagoya University, Furo-cho, Chikusa-ku, Nagoya, Aichi 464-8601, Japan.*

[c] *Department of Materials Process Engineering, Nagoya University, Furo-cho, Chikusa-ku, Nagoya, Aichi 464-8603, Japan.*

[d] *Faculty of Pharmacy and Pharmaceutical Sciences, Josai University, 1-1 Keyakidai, Sakado, Saitama 350-0295, Japan.*

[e] *Institute for Research on Next-generation Semiconductor and Sensing Science (IRES²), Toyohashi University of Technology, 1-1 Hibarigaoka, Tempaku-cho, Toyohashi, Aichi 441-8580, Japan.*

[f] *National Research Institute of Police Science, 6-3-1 Kashiwanoha, Kashiwa, Chiba 277-0882, Japan.*

*Corresponding authors:

Akira Miyajima (miyajima.akira.ci@tut.jp), Takayuki Shibata (shibata@me.tut.ac.jp)

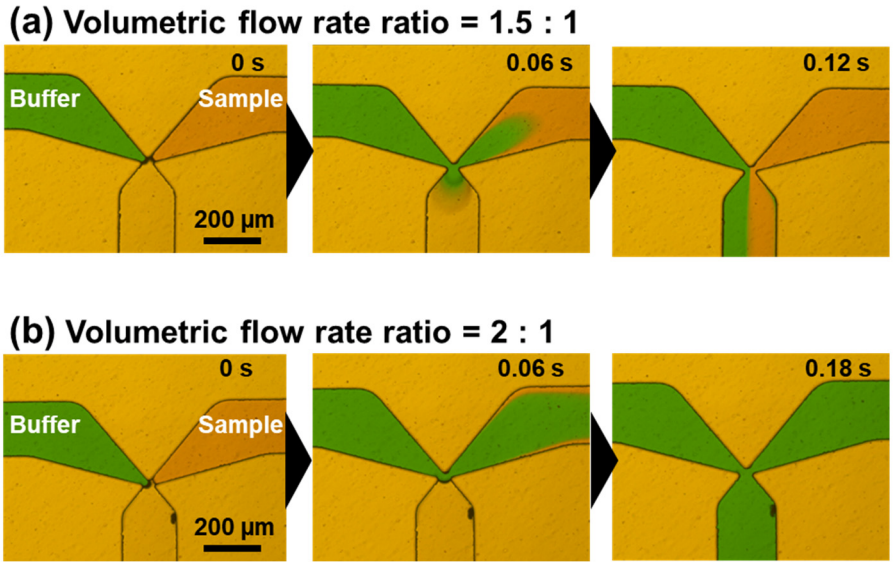


**Fig. S1** Experimental results showing the flow behavior of two liquids at the Y-junction microchannel (200 and 100 μm in width and height, respectively), with a minimum width of 32 μm at the constricted region. Volumetric flow rate ratios of (a) 1.5:1 and (b) 2:1. At a flow rate ratio of 1.5:1, the two liquids flowed into the downstream microchannel below the confluence point within 0.06 s. The dilution buffer slightly backflowed into the sample side. Conversely, at a flow rate ratio of 2:1, the dilution buffer flowed into the sample side after merging and then the sample liquid eventually pushed it back, forming a stable laminar flow in the downstream microchannel after approximately 3 s.

## S1. Theoretical burst pressure of passive stop valves

As shown in Fig. S2, when the cross-sectional area of a microchannel expands suddenly, the liquid is pinned near the outlet owing to surface tension. To simplify the theoretical model, assume that the corner radii are $r_1 = r_2 = r$ (i.e., $\beta_1 = \beta_2 = \beta$) and $r_3 = 0$ (i.e., $\beta_3 = 0$) due to considerations of pattern accuracy in the photolithography process. The theoretical burst pressure at the confluent point of a two-heighted Y-junction is described as follows[1,2]:

$$P_1 = -\gamma\left(\frac{2\cos\left(\min(\theta_m + \beta, 180°)\right)}{g + 2r(1 - \cos\beta)} + \frac{\cos(\theta_m + 90°) + \cos\theta_f}{H - h}\right) \quad (1)$$

where $g$ (32 μm) represents the minimum width of the microchannel at the confluent point, $H$ (90 μm) and $h$ (10 μm) denote the heights of the microchannels, $\vartheta_m$ is the contact angle of water on the surfaces of the top and sidewalls of the microchannel at the narrow gap (i.e., $\vartheta_m$ = 108° for PDMS), $\vartheta_f$ is the contact angle of water on the bottom surface of the microchannel (namely, $\vartheta_f$ = 102° for silicone-based adhesive double-sided tape), $\gamma$ is the surface tension of the liquid ($\gamma$ = 0.073 N/m for water), $r$ (5 μm) is the radius of the rounded corner, and $\beta$ is the angle between the direction perpendicular to the longitudinal direction of the microchannel and the position of the liquid–air meniscus, which is pinned at the rounded corner. According to the theory, the theoretical burst pressure at a two-heighted Y-junction was estimated to be $P_1$ = 12.7 kPa for water.

Similarly, as there is no step in the microchannel height, the burst pressure at the outlet of each microchamber is simplified from eqn (1) as follows:

$$P_2 = -\gamma\left(\frac{2\cos\left(\min(\theta_m + \beta, 180°)\right)}{g + 2r(1 - \cos\beta)} + \frac{\cos\theta_m + \cos\theta_f}{h}\right) \quad (2)$$

where $g$ (20 μm) and $h$ (10 μm) represent the minimum width and height of the microchannel, respectively and $r$ (5 μm) is the radius of the convex rounded corner. According to eqn (2), the theoretical burst pressure of a permanent stop valve at the outlet of each microchamber was estimated to be $P_2$ = 9.5 kPa for water.

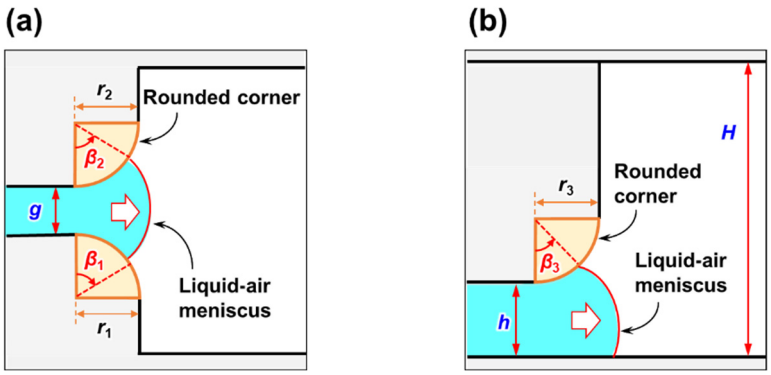


**Fig. S2** Theoretical model describing the burst pressure. (a) Plan and (b) cross sectional views of the liquid-air meniscus pinned on the back edge of the convex rounded corner.

## References


1 D. Natsuhara, R. Saito, H, Aonuma, T. Sakurai, S. Okamoto, M. Nagai, H. kanuka and T. Shibata, *Lab Chip*, 2021, **21**, 4779-4790, DOI: 10.1039/d1lc00829c.

2 D. Natsuhara, S. Misawa, R. Saito, K. Shirai, S. Okamoto, M. Nagai, M. Kitamura and T. Shibata, *Sci. Rep.*, 2022, **12**, 12852, DOI: 10.1038/s41598-022-16945-2.

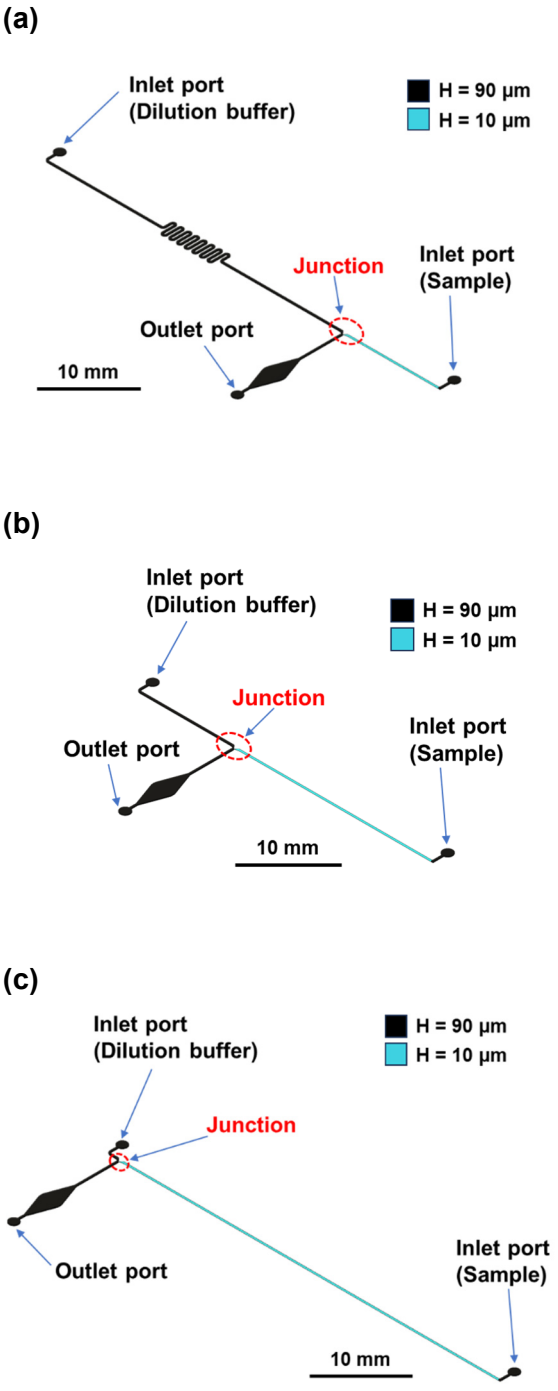


**Fig. S3** Schematic diagram of the microfluidic device with a microchannel width of 200 μm and microchannel heights of 90 and 10 μm on the dilution buffer and sample sides, respectively, designed to evaluate (a) 100-fold, (b) 1,000-fold, and (c) 10,000-fold dilutions of two liquids passing through the two-heighted Y-junction.

## S2. Theory for generating logarithmic dilution factors in the microfluidic device

To generate logarithmic dilutions across four orders of magnitude (10–10,000-fold) in the microfluidic device, the flow resistance ratios of microchannels should be optimized for each dilution factor. The theoretical flow resistance *R* in a rectangular microchannel is expressed by[1]:

$$R = \frac{12\eta L}{H^3 W}\left(1 - 0.630\frac{H}{W}\right)^{-1} \quad (3)$$

where *W*, *H*, and *L* represent the microchannel's width, height, and length, respectively, and $\eta$ is the dynamic viscosity of the liquid ($\eta$ = 1 mPa·s for water). Therefore, the flow resistance can be adjusted by the microchannel's height *H* and length *L* under a constant microchannel width (*W* = 200 μm) (Figs. 2 and S3). Additionally, the theoretical volumetric flow rate *Q* can be estimated as follows:

$$Q = \frac{\Delta P}{R} \quad (4)$$

where the theoretical pressure drop Δ*P* is equivalent to the applied pressure, which is adjusted by two pressure-controlled micropumps in the two-liquid merging experiments. The calculated theoretical volumetric flow rates of the dilution buffer and sample solutions at each dilution factor at a constant pressure (Δ*P* = 3.5 kPa) are listed in Table S1. The designed microchannel layout enables the correct flow resistance ratio from the inlet ports to the confluent point on the dilution buffer and sample sides for each dilution factor.

## Reference

1 D. Natsuhara, R. Saito, H, Aonuma, T. Sakurai, S. Okamoto, M. Nagai, H. kanuka and T. Shibata, *Lab Chip*, 2021, **21**, 4779-4790, DOI: 10.1039/d1lc00829c.

**Table S1** Theoretical volumetric flow rates of the dilution buffer and sample solutions at each dilution factor at a constant pressure ($\Delta P$ = 3.5 kPa).

(a) Characteristics of the 10-fold dilution factor in the device as shown in Fig. 2.

| | Dilution buffer | Sample | |
|---|---|---|---|
| Microchannel height *H* (μm) | 90 | 90 | 10 |
| Microchannel length *L* (mm) | 299.73 | 1.00 | 5.00 |
| Flow resistance *R* (kPa·min/μL) | $5.74 \times 10^{-1}$ | $1.91 \times 10^{-3}$ | 5.16 |
| Volumetric flow rate *Q* (μL/min) | 6.10 | 0.68 | |
| Flow rate ratio [a] | 9.0 | 1.0 | |

(b) Characteristics of the 100-fold dilution factor in the device as shown in Fig. S3a.

| | Dilution buffer | Sample | |
|---|---|---|---|
| Microchannel height *H* (μm) | 90 | 90 | 10 |
| Microchannel length *L* (mm) | 54.50 | 1.00 | 10.00 |
| Flow resistance *R* (kPa·min/μL) | $1.04 \times 10^{-1}$ | $1.91 \times 10^{-3}$ | $1.03 \times 10^{1}$ |
| Volumetric flow rate *Q* (μL/min) | 33.54 | 0.34 | |
| Flow rate ratio [a] | 99.0 | 1.0 | |

(c) Characteristics of the 1,000-fold dilution factor in the device as shown in Fig. S3b.

| | Dilution buffer | Sample | |
|---|---|---|---|
| Microchannel height *H* (μm) | 90 | 90 | 10 |
| Microchannel length *L* (mm) | 10.80 | 1.00 | 20.00 |
| Flow resistance *R* (kPa·min/μL) | $2.07 \times 10^{-2}$ | $1.91 \times 10^{-3}$ | $2.07 \times 10^{1}$ |
| Volumetric flow rate *Q* (μL/min) | 169.30 | 0.17 | |
| Flow rate ratio [a] | 999.0 | 1.0 | |

(d) Characteristics of the 10,000-fold dilution factor in the device as shown in Fig. S3c.

| | Dilution buffer | Sample | |
|---|---|---|---|
| Microchannel height *H* (μm) | 90 | 90 | 10 |
| Microchannel length *L* (mm) | 2.16 | 1.00 | 40.00 |
| Flow resistance *R* (kPa·min/μL) | $4.13 \times 10^{-3}$ | $1.91 \times 10^{-3}$ | $4.13 \times 10^{1}$ |
| Volumetric flow rate *Q* (μL/min) | 847.15 | 0.08 | |
| Flow rate ratio [a] | 9997.1 | 1.0 | |

[a] The flow rate ratios were calculated using the values of the volumetric flow rates before rounding to the second decimal place.

## Reference

1 E. Yildirim, S. J. Trietsch, J. Joore, A. van den Berg, T. Hankemeiera and P. Vulto, *Lab Chip*, 2014, **14**, 3334-3340, DOI: 10.1039/C4LC00261J.

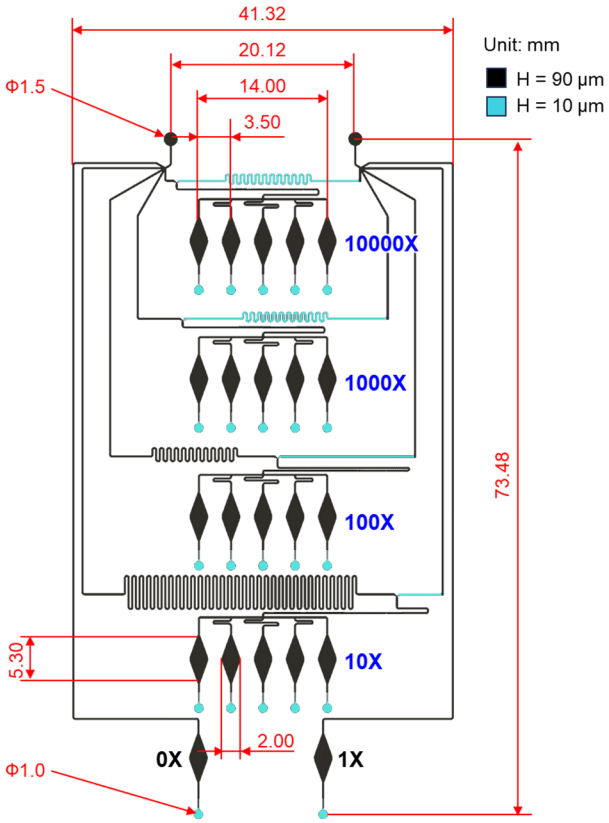


**Fig. S4** Detailed design of the four-stepwise logarithmic parallel dilution microfluidic device (10–10,000-fold) in a single operation. Each dilution factor was generated independently in a parallel microchannel network at a constant pressure.

**Table S2** Theoretical volumetric flow rates of the dilution buffer and sample solutions at each dilution factor at a constant pressure ($\Delta P$ = 7.0 kPa) in the four-stepwise logarithmic dilution device (Fig. S4).

(a) Characteristics of the 10-fold dilution factor.

| | Dilution buffer | Sample | |
|---|---|---|---|
| Microchannel height *H* (μm) | 90 | 90 | 10 |
| Microchannel length *L* (mm) | 305.66 | 54.91 | 5.00 |
| Flow resistance *R* (kPa·min/μL) | $5.85 \times 10^{-1}$ | $1.05 \times 10^{-1}$ | 5.16 |
| Volumetric flow rate *Q* (μL/min) | 11.96 | 1.33 | |
| Flow rate ratio [a] | 9.0 | 1.0 | |

(b) Characteristics of the 100-fold dilution factor.

| | Dilution buffer | Sample | |
|---|---|---|---|
| Microchannel height *H* (μm) | 90 | 90 | 10 |
| Microchannel length *L* (mm) | 82.05 | 34.45 | 15.00 |
| Flow resistance *R* (kPa·min/μL) | $1.57 \times 10^{-1}$ | $6.60 \times 10^{-2}$ | $1.55 \times 10^{1}$ |
| Volumetric flow rate *Q* (μL/min) | 44.56 | 0.45 | |
| Flow rate ratio [a] | 99.0 | 1.0 | |

(c) Characteristics of the 1,000-fold dilution factor.

| | Dilution buffer | Sample | |
|---|---|---|---|
| Microchannel height *H* (μm) | 90 | 90 | 10 |
| Microchannel length *L* (mm) | 21.61 | 16.80 | 40.00 |
| Flow resistance *R* (kPa·min/μL) | $4.14 \times 10^{-2}$ | $3.22 \times 10^{-2}$ | $4.13 \times 10^{1}$ |
| Volumetric flow rate *Q* (μL/min) | 169.19 | 0.17 | |
| Flow rate ratio [a] | 999.1 | 1.0 | |

(d) Characteristics of the 10,000-fold dilution factor.

| | Dilution buffer | Sample | |
|---|---|---|---|
| Microchannel height *H* (μm) | 90 | 90 | 10 |
| Microchannel length *L* (mm) | 2.16 | 1.00 | 40.00 |
| Flow resistance *R* (kPa·min/μL) | $4.13 \times 10^{-3}$ | $1.91 \times 10^{-3}$ | $4.13 \times 10^{1}$ |
| Volumetric flow rate *Q* (μL/min) | 1694.30 | 0.17 | |
| Flow rate ratio [a] | 9997.1 | 1.0 | |

[a] The flow rate ratios were calculated using the values of the volumetric flow rates before rounding to the second decimal place.

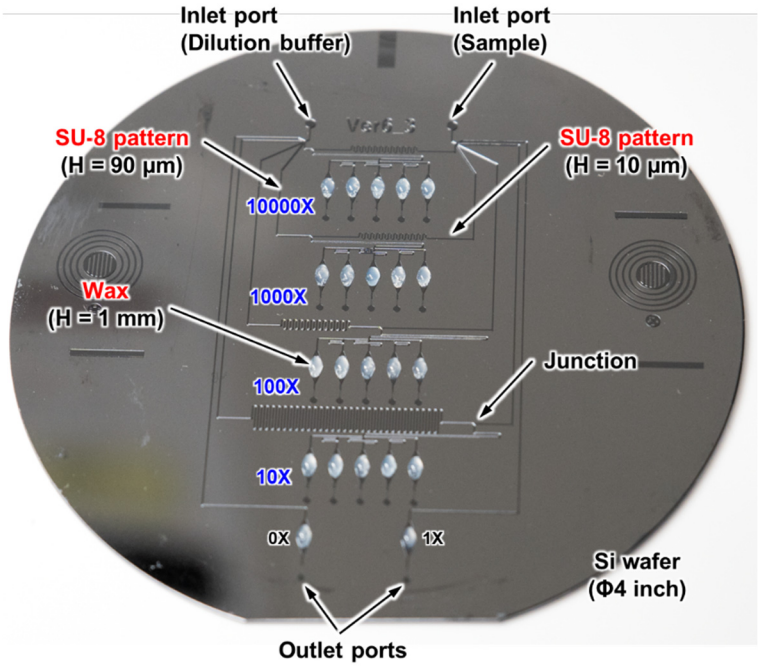


**Fig. S5** Master mold fabricated on a 6-inch Si wafer consisting of two main parts: SU-8 microchannel patterns with heights of 10 and 90 μm on the sample and dilution buffer sides, respectively, and semi-ellipsoid-shaped wax structures with a uniform shape that create deep localized microchambers (up to 1 mm in depth).

**Table S3** Components and volumes used for colorimetric LAMP assays in the four-stepwise logarithmic parallel dilution microfluidic device. Each microchamber has 3 µL of volume.

| Component | Concentration | Volume (µL) |
|---|---|---|
| 2× Reaction mixture | – | 62.5 |
| *Bst* DNA polymerase | 8 U/µL | 5.0 |
| DNA template | 10 ng/µL (Cannabis seed)<br>8 ng/µL (Cannabis resin) | (20–30) [a] |
| Primer | FIP 30.8 pmol<br>BIP 30.8 pmol<br>F3 3.8 pmol<br>B3 3.8 pmol<br>LF 15.4 pmol<br>LB 15.4 pmol | 6.5 |
| Hydroxynaphthol blue | 4.2 mM | 4.48 |
| Distilled water | – | 34.02 |
| Total | | 112.5 [b] |

[a] The DNA template was introduced into the device separately from the LAMP reagents through a different inlet port.

[b] Total volume does not include the volume of the DNA template.

**Table S4** Components and volumes used for conventional off-chip LAMP assays for a cannabis seed performed using a real-time turbidimeter.

| **Component** | Concentration | Volume (µL) |
|---|---|---|
| 2× Reaction mixture | – | 12.5 |
| *Bst* DNA polymerase | 8 U/µL | 1.0 |
| DNA template | 1–1000 pg/µL<br>(Cannabis seed) | 2.5 |
| Primer | FIP 30.8 pmol<br>BIP 30.8 pmol<br>F3 3.8 pmol<br>B3 3.8 pmol<br>LF 15.4 pmol<br>LB 15.4 pmol | 1.3 |
| Distilled water | – | 7.7 |
| Total | | 25.0 |

**Table S5** Components and volumes used for conventional real-time fluorescent LAMP assays for a cannabis resin performed using EvaGreen® dye as a fluorescent indicator.

| **Component** | Concentration | Volume (μL) |
|---|---|---|
| 2× Reaction mixture | – | 12.5 |
| *Bst* DNA polymerase | 8 U/μL | 1.0 |
| DNA template | 1–1000 pg/μL (Cannabis resin) | 2.5 |
| Primer | FIP 30 pmol<br>BIP 30 pmol<br>F3 5 pmol<br>B3 5 pmol<br>LF 15 pmol<br>LB 15 pmol | 1.3 |
| EvaGreen® dye | 25 μM | 1.25 |
| Distilled water | – | 6.45 |
| Total | | 25.0 |

**Table S6** Components and volumes used for real-time PCR assays for a cannabis resin performed using EvaGreen® dye as a fluorescent indicator.

| **Component** | Concentration | Volume (μL) |
|---|---|---|
| *Taq* 2× Master Mix | – | 10.0 |
| DNA template | 1–1000 pg/μL (Cannabis resin) | 2.0 |
| Forward primer | 10 μM | 0.5 |
| Reverse primer | 10 μM | 0.5 |
| EvaGreen® dye | 25 μM | 1.0 |
| Distilled water | – | 6.0 |
| Total | | 20.0 |

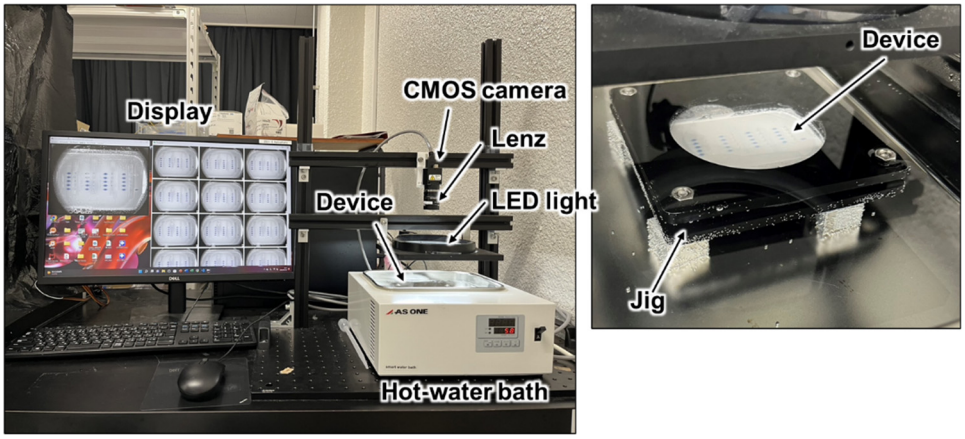


**Fig. S6** Schematic of the homebuilt time-lapse imaging equipment and the dilution device mechanically clamped with a jig. (a) Photograph of the time-lapse imaging equipment. (b) Photograph of the device clamped with a jig immersed in a hot-water bath during the LAMP assay.

**Table S7** Absorbance measurements of the diluted solutions generated at each dilution factor. Mean and standard deviation (SD) values were calculated from five experiment replicates for the device dilution, whereas only a single replicate was performed for the manual dilution.

| Dilution factor | | 10X | 100X | 1000X | 10000X |
|---|---|---|---|---|---|
| Manual dilution | | 50.550 | 7.625 | 0.858 | 0.091 |
| Device dilution | Mean value | 29.198 | 3.138 | 0.824 | 0.147 |
| | standard deviation | 0.132 | 0.044 | 0.019 | 0.014 |

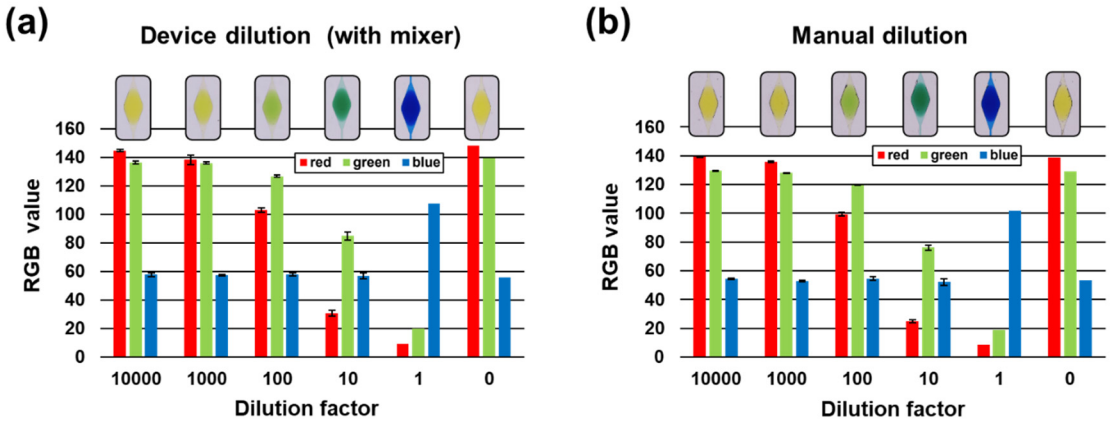


**Fig. S7** Results of image analysis of the mean RGB values obtained from five microchambers at each dilution factor. (a) Device dilution with the micromixer. (b) Manual dilution.

**Table S8** Comparison of the R/G values between device-based dilutions with the micromixer and manually prepared dilutions. Mean and standard deviation (SD) values were calculated from five experiment replicates for the device dilution and the manual dilution.

| Dilution factor | | 10X | 100X | 1000X | 10000X |
|---|---|---|---|---|---|
| Manual dilution | Mean value | 0.327 | 0.830 | 1.062 | 1.075 |
| | standard deviation | 0.007 | 0.008 | 0.002 | 0.001 |
| Device dilution | Mean value | 0.359 | 0.813 | 1.016 | 1.061 |
| | standard deviation | 0.011 | 0.010 | 0.021 | 0.003 |

**Table S9** Tt values obtained from the colorimetric LAMP assay for a cannabis seed using the four-stepwise logarithmic parallel dilution microfluidic device. Each microchamber has 3 μL of volume.

| Dilution factor | 10X | 100X | 1000X | 10000X |
|---|---|---|---|---|
| DNA concentration (copies/μL) | $1.04 \times 10^3$ | $1.04 \times 10^2$ | $1.04 \times 10^1$ | $1.04 \times 10^0$ |
| Tt value (min) | | | | |
| Chamber No. 1 | 19.5 | 28.9 | 32.2 | n.d. |
| Chamber No. 2 | 22.7 | 25.4 | 31.3 | 43.4 |
| Chamber No. 3 | 22.6 | 28.9 | 27.8 | n.d. |
| Chamber No. 4 | 20.5 | 25.9 | 29.2 | (53.5) [a] |
| Chamber No. 5 | 23.0 | 24.4 | 38.7 | n.d. |
| Mean value | 21.7 | 26.7 | 31.8 | 43.4 |
| Standard deviation | 1.6 | 2.1 | 4.2 | — |

[a] As the Tt value exceeded 50 min, it was excluded from the data due to the possibility of a false positive.

**Table S10** Tt values obtained from conventional off-chip LAMP assays for a cannabis seed using a real-time turbidimeter in a 25-μL reaction volume.

| Dilution factor | 10X | 100X | 1000X | 10000X |
|---|---|---|---|---|
| DNA concentration (copies/μL) | $1.04 \times 10^3$ | $1.04 \times 10^2$ | $1.04 \times 10^1$ | $1.04 \times 10^0$ |
| Tt value (min) | | | | |
| Experiment No. 1 | 20.8 | 23.3 | 27.8 | n.d. |
| Experiment No. 2 | 21.3 | 24.7 | 30.6 | 32.4 |
| Experiment No. 3 | 22.0 | 24.6 | 29.7 | n.d. |
| Mean value | 21.4 | 24.2 | 29.4 | 32.4 |
| Standard deviation | 0.6 | 0.8 | 1.4 | — |

**Table S11** Tt values obtained from the colorimetric LAMP assay for a cannabis resin using the four-stepwise logarithmic parallel dilution microfluidic device. Each microchamber has 3 µL of volume.

| Dilution factor | 10X | 100X | 1000X | 10000X |
|---|---|---|---|---|
| DNA concentration (copies/µL) | $0.83 \times 10^3$ | $0.83 \times 10^2$ | $0.83 \times 10^1$ | $0.83 \times 10^0$ |
| Tt value (min) | | | | |
| Chamber No. 1 | n.d. | 38.0 | 25.8 | 22.3 |
| Chamber No. 2 | n.d. | 36.5 | 25.6 | 22.8 |
| Chamber No. 3 | n.d. | 31.2 | 25.3 | 22.9 |
| Chamber No. 4 | n.d. | 33.0 | 25.1 | 22.4 |
| Chamber No. 5 | n.d. | 37.2 | 25.7 | 25.8 |
| Mean value | — | 35.2 | 25.5 | 23.2 |
| Standard deviation | — | 2.9 | 0.3 | 1.5 |

[a] As the Tt value exceeded 50 min, it was excluded from the data due to the possibility of a false positive.

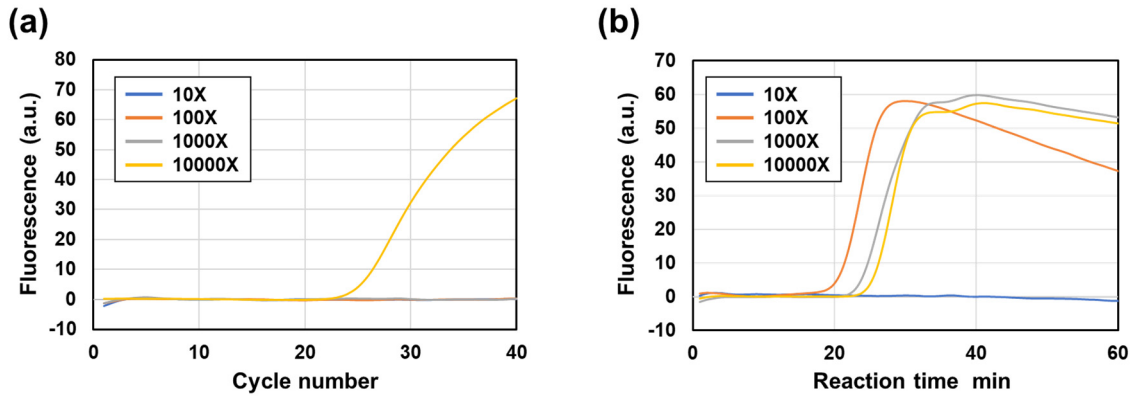


**Fig. S8** DNA amplification curves of cannabis resin DNA samples prepared at dilution factors from 10- to 10,000-fold using (a) real-time PCR (20-µL reaction volume) and (b) real-time fluorescent LAMP (25-µL reaction volume).